Performance of biochar derived from rice straw for removal of Ni(II) in batch experiments

Lijia Dong, Wensheng Linghu, Donglin Zhao, Yinyan Mou, Baowei Hu, Abdullah M. Asiri, Khalid A. Alamry, Di Xu and Jin Wang

ABSTRACT

Biochar, as a cost-efficient adsorbent, is of major interest in the removal of heavy metals from wastewater. Herein, batch experiments were conducted to investigate the performance of biochar derived from rice straw for the removal of Ni(II) as a function of various environmental conditions. The results showed that Ni(II) sorption was strongly dependent on pH but independent of ionic strength and the effects of electrolyte ions could be negligible over the whole pH range. Ionic exchange and inner-sphere surface complexation dominated the sorption of Ni(II). Humic/fulvic acids clearly enhanced the Ni(II) sorption at pH <7.2 but inhibited the sorption at pH >7.2. The sorption reached equilibrium within 10 hours, and the kinetics followed a pseudo-second-order rate model. Any of the Langmuir, Freundlich, or Dubinin-Radushkevich isotherm models could describe the sorption well, but the Langmuir model described it best. The maximum sorption capacity calculated from the Langmuir model was 0.257 m·mol/g. The thermodynamic parameters suggested that Ni(II) sorption was a spontaneous and endothermic process and was enhanced at high temperature. The results of this work indicate that biochar derived from rice straw may be a valuable bio-sorbent for Ni(II) in aqueous solutions, but it still requires further modification.

Key words | biochar, HA/FA, Ni(II), sorption, thermodynamic parameters

Lijia Dong
Yinyan Mou
Baowei Hu (corresponding author)
School of Life Sciences,
Shaoxing University,
Huancheng West Road 508, Shaoxing,
Zhejiang 312000, China
E-mail: *hbw@usx.edu.cn*

Wensheng Linghu
School of Chemistry and Chemical Engineering,
Shaoxing University,
Huancheng West Road 508, Shaoxing,
Zhejiang 312000, China

Donglin Zhao
School of Materials and Chemical Engineering,
Anhui University of Architecture,
Hefei 230601, China

Abdullah M. Asiri
Khalid A. Alamry
Chemistry Department, Faculty of Science,
King Abdulaziz University,
Jeddah 21589, Saudi Arabia

Di Xu
State Key Laboratory of Lake Science and Environment,
Nanjing Institute of Geography and Limnology, CAS,
Nanjing 210008, China

Jin Wang
College of Environmental Science and Engineering,
Guangzhou University,
Guangzhou 510006, China

INTRODUCTION

Currently, increasing amounts of industrial and agricultural effluents are discharged into the environment, resulting in more inorganic and organic pollution of soil and water. Most organic pollutants are biodegradable, but inorganic pollutants, especial heavy metals, are non-biodegradable and can be accumulated through the human and animal food chains. This accumulation of heavy metals is a serious threat to human health, aquatic organisms and ecological safety over a long period (Dong *et al.* 2014). Nickel (Ni) mainly derives from steel factories, batteries manufacturing, and metal and alloy production (Gautam *et al.* 2015). It is well known that as a micronutrient, Ni is part of the synthesis of vitamin B12, and an activator in some enzyme systems. However, high dosages can cause serious diseases such as hepatitis, nephritic syndrome, anaemia, and diarrhoea (Kasprzak *et al.* 2003). It is therefore necessary to reduce ionic Ni to permissible limits before its discharge into the natural environment.

The United States Environmental Protection Agency (EPA) provides current maximum allowable contaminant levels for many heavy metals. To meet the EPA standards, various removal techniques such as ion exchange,

doi: 10.2166/wst.2018.238

precipitation, sorption, and electrocoagulation are used in sewage treatment (Inyang *et al.* 2015). Among these techniques, the sorption approach has been extensively adopted due to its ease of operation, low cost, and high efficiency. However, different adsorbents exhibit different sorption abilities. For instance, the sorption behaviours of Ni on a series of adsorbents, including activated carbon (Kadirvelu *et al.* 2001), clays (Gupta & Bhattacharyya 2006), Na-attapulgite (Fan *et al.* 2009), carbon nanotubes (Chen *et al.* 2009), mordenite (Yang *et al.* 2011), magnetic nanoparticles (Panneerselvam *et al.* 2011), graphene oxides (Chen *et al.* 2016a), and montmorillonite (Chen *et al.* 2016b) showed a large variation. Not only that, many feedstock materials in nature have the potential to be cost-efficient adsorbents. Thus, potential adsorbents deserve further exploration.

Biochar can be produced from agricultural residues, the majority of which are waste or by-products from the harvesting and processing of crops (Inyang *et al.* 2015). Thus, there are dual benefits for environmental protection to utilize agricultural wastes as adsorbents for the removal of heavy metals. Furthermore, many low-cost adsorbents have been used to remove contaminants from water, such as tea factory waste (Malkoc & Nuhoglu 2005), diatomite (Sheng *et al.* 2011), sepiolite (Liang *et al.* 2011), diatoms and algae (Bird *et al.* 2011), peat (Zhou *et al.* 2012), coke plant wastewaters (Zhou *et al.* 2017), and zeolite (Ciosek & Luk 2017), which are widely applied to adsorb metal ions and other pollutants from water. It is therefore important to study these kinds of low-cost adsorbents. In this paper, we selected the residual wastes of *Oryza sativa*, which are scarcely utilized in the field, as a feedstock to obtain biochar through pyrolysis techniques. The sorption properties of this biochar for heavy metals in water are rarely reported. For these reasons, the sorption of Ni(II) on biochar derived from rice straw was investigated under various experimental conditions including contact time, pH, ionic strength, foreign cations and anions, solid content, and temperature. The sorption kinetics was simulated by a pseudo-second-order model to illustrate the possible kinetic interaction mechanism. The equilibrium sorption behaviour of biochar was studied using sorption isotherms. Experimental data were fitted to the Langmuir, Freundlich, and Dubinin-Radushkevich (D-R) models to determine the interaction mechanism between Ni(II) and biochar. The thermodynamics of the sorption process was also investigated to demonstrate the characteristics of Ni(II) sorption on biochar. This exploration for the sorption capacity and underlying mechanisms of rice straw-derived biochar will improve its long-term performance in field applications.

EXPERIMENTAL

Materials

Rice straw, one of the most common agricultural residues, was selected as the feedstock for biochar in this research. Specifically, the aboveground biomass of *Oryza sativa* L. without seeds was acquired from farmlands in Shaoxing, Zhejiang province, China. Then, the individual plants were washed with tap water, air dried in a hot-air oven at 80°C for 12 hours, crushed, and ground to <1.0 mm particle size using a fodder grinder. Finally, the ground particles were slowly pyrolysed at 600°C in a pyrolyser without admission of air for 2 hours at a heating rate of 7°C/min. All biochar samples were cooled to room temperature and stored in desiccators before use.

A stock solution of Ni ions was prepared by dissolving $Ni(NO_3)_2{\cdot}6H_2O$ in deionized water. All reagents used in this experiment were of analytical grade with a mass fraction purity of 0.99 and underwent no further purification.

We obtained humic acid (HA) and fulvic acid (FA) by extracting them from the soil in Hua-Jia County (Gansu province, China). It has been proved that both HA and FA are ubiquitous in aquatic environments and have all kinds of functional groups that allow HA and FA to complex with heavy metals and to interact with adsorbents, which finally influences the sorption and transportation of heavy metal by adsorbents (Tang *et al.* 2013).

Characterization of biochar

Both scanning electron microscopy (SEM) images and transmission electron microscopy (TEM) images of biochar derived from rice straw were obtained using a field emission scanning electron microscope (JSM-6360LV, Japan) and a transmission electron microscope (JEM-1011, Japan), respectively. Simultaneously, the biochar sample was characterized using a Fourier transform infrared (FTIR) spectrometer (NEXUS, USA) in the wavenumber range of 4,000–400 cm^{-1}. A spectral resolution of 2 cm^{-1} and an energy ratio range of 25–40% were set up to determine the surface functional groups of the biochar.

Batch sorption experiments

The sorption behaviour of biochar from rice straw for Ni(II) was investigated by batch adsorption experiments at three temperatures, i.e., 293 K, 313 K, and 333 K. Briefly, the

stock suspensions of Ni(II) ions solution, biochar, $NaClO_4$, $KClO_4$, $LiClO_4$, $NaNO_3$, NaCl, HA, FA, and Milli-Q water were added to polyethylene tubes in order to obtain the desired concentrations of the different constituents. The solution pH was adjusted with 0.01 or 0.1 M $HClO_4$ or NaOH solutions. The batch experiments were carried out in 15 mL polyethylene tubes using the desired pH value, ionic strength, coexisting electrolyte ions, contact time, and temperature. The ratio of the amount of biochar to the solution volume was 0.45 g/L. After the equilibrium time, the solid and liquid phases were separated by centrifugation at 9,000 rpm for 30 min. The concentration of Ni(II) in the supernatant was measured with a Shimadzu 6,300 atomic adsorption spectrophotometer (Japan).

All experiments were run in duplicate or triplicate and the experimental data were averaged to ensure experimental repeatability and improve data accuracy. The relative errors of the experimental data were less than 5%. The Ni(II) removal efficiency by biochar [Ni(II) sorption (%) $= (C_0 - C_e)/C_0 \times 100$], distribution coefficient [$K_d = (C_0 - C_e)/C_e \times V/m$], and sorption amount onto biochar [$q_e = (C_0 - C_e) \times V/m$] were calculated from the initial Ni(II) concentration (C_0, mol/L), the final or equilibrium Ni(II) concentration (C_e, mol/L), the biochar mass (m, g), and the suspension volume (V, L).

RESULTS AND DISCUSSION

Characterization of biochar

The SEM and TEM images for biochar are shown in Figure 1. Both images show the irregularly porous structure of biochar. The SEM image (Figure 1(a)) shows that the surface and the edge of biochar are rough and various blocky structures randomly pile up. The TEM image (Figure 1(b)) also shows the loose inner structure of biochar. All these characteristics may endow the rice straw-derived biochar

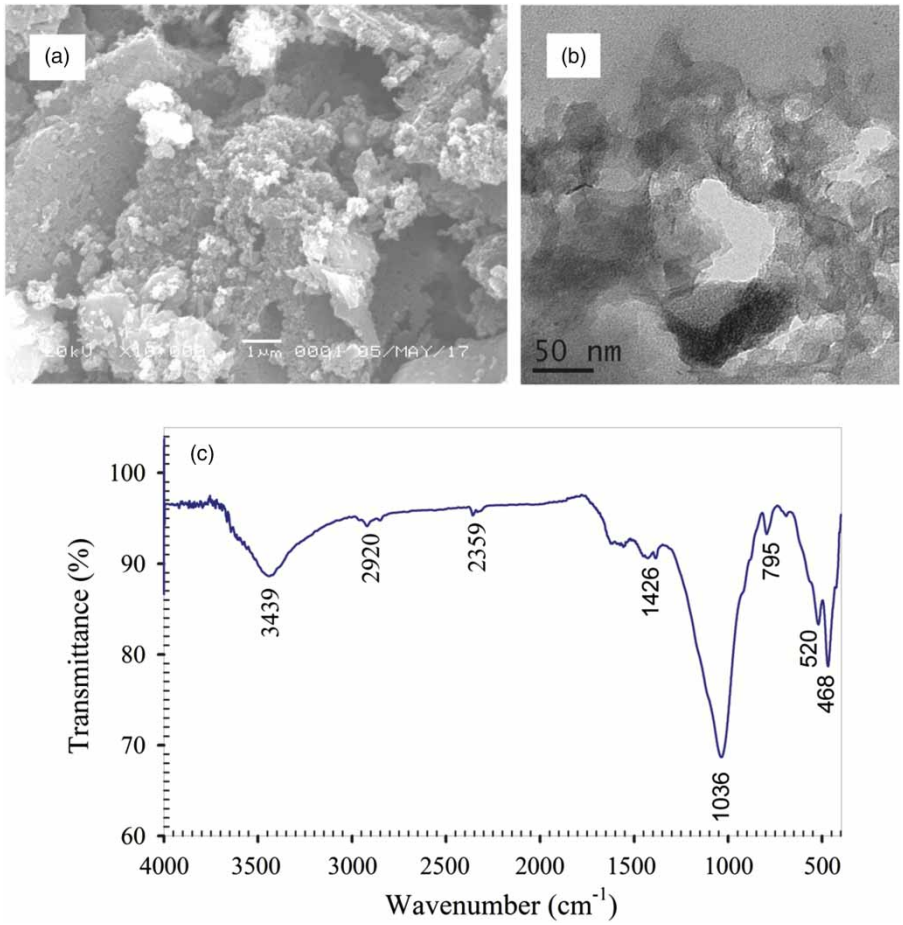

Figure 1 | SEM image (a), TEM image (b) and FTIR spectrum (c) of biochar derived from rice straw.

with favourable sorption abilities. The FTIR spectrum of biochar is shown in Figure 1(c). The broad band at 3,439 cm^{-1} is attributed to the O-H stretching vibration of biochar (Tong *et al.* 2011; Kołodyńska *et al.* 2017). The peaks at 1,426 and 1,036 are assigned to carboxyl O= *C*−O and alkoxy C−O stretching vibrations, respectively (Hu *et al.* 2017a). The bands at 795, 520, and 468 may be assigned to the integrated crystalline structure of biochar (Zong *et al.* 2013), which needs to be further studied.

Effect of contact time

The effect of contact time on Ni(II) sorption by biochar and the ratio of t to q_t is shown in Figure 2. It is evident that the amount of Ni(II) adsorbed on biochar rapidly increases during the initial 5 hours of contact time, and then the sorption rate slows down until equilibrium is reached. The occurrence of fast sorption during the initial contact time may arise from the availability of large numbers of sites on the biochar surface. With the sites gradually being occupied, the kinetic rate of sorption becomes slower. The mechanisms may involve the less reactive sites on the biochar surface, diffusion into internal sites, and the formation of complexes or precipitation (Chen *et al.* 2016b). These results imply that the sorption of Ni(II) on biochar is a chemical but not a physical process. In addition, considering the kinetic rates, 24 hours of stirring time was selected to assure that the sorption completely reached equilibrium in the batch experiments.

To study the specific rate constant of Ni(II) sorption on biochar, pseudo-second-order models were used to fit the data. The linear form of the pseudo-second order kinetic was calculated as follows (Ho & McKay 1999; Ho 2006):

$$\frac{t}{q_t} = \frac{1}{2kq_e^2} + \frac{t}{q_e} \quad (1)$$

where q_e and q_t represent the Ni(II) sorption ability (mol/g) at equilibrium time and time t (h), respectively; and k [g/(mol·h)] is the rate constant. As shown in Figure 2, there is an extremely significant linear relationship between t/q_t and t ($r^2 = 0.995$, $P < 0.001$), suggesting that the kinetic sorption process can be well described by a pseudo-second-order rate equation. This result indicates that the sorption of Ni(II) onto biochar is a chemical process, which is also the rate-limiting step.

Effect of the initial pH and ionic strength of solutions

The pH of a solution can influence functional groups on the adsorbent surface and the species of an adsorbate (Chen *et al.* 2016a), and thus pH plays a key role in the sorption process. The effect of the initial pH on Ni(II) sorption with 0.001, 0.01, and 0.1 $NaClO_4$ solutions is shown in Figure 3. It is obvious that the sorption of Ni(II) on biochar derived from rice straw is strongly affected by the initial pH values of the solutions at pH <8.8. In addition, the sorption percentage increases with increasing pH, but the sorption curve over the whole pH range here can be divided into three regions: (1) the sorption slowly increases from approximately 8% to 16% over the pH range from 4 to 6; (2) the sorption rapidly increases from 16% to a maximum value of 90% over the pH range from 6 to 8.8; and (3) the sorption percentage maintains its highest level at pH >8.8.

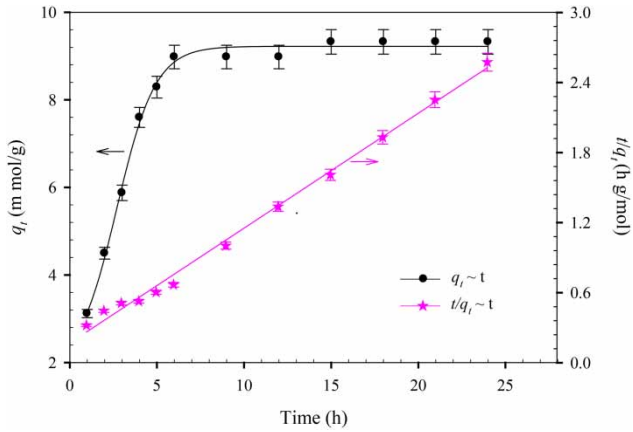

Figure 2 | Time dependence of Ni(II) sorption on biochar and pseudo-second-order rate calculation of Ni(II) sorption on biochar. $T = 293 \pm 2$ K, pH = 6.0 ± 0.2, I ($NaClO_4$) = 0.01 mol/L, m/V = 0.45 g/L.

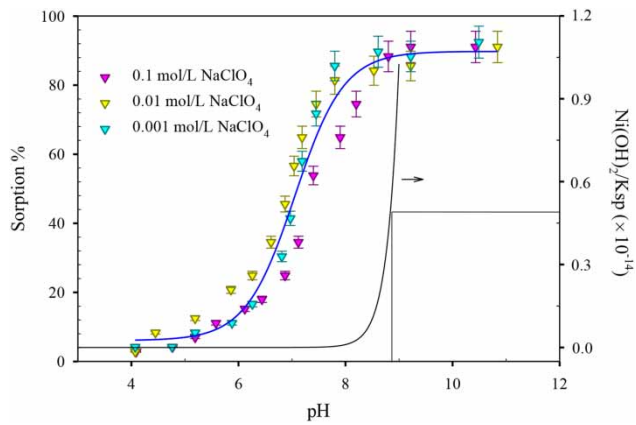

Figure 3 | Effect of pH and ionic strength on Ni(II) sorption on biochar surface. $T = 293 \pm 2$ K, $C_{Ni(II)initial}$ = 10 mg/L, m/V = 0.45 g/L.

A similar sorption curve was found in Ni(II) sorption on montmorillonite (Chen *et al.* 2016b). This result suggests that the sorption of Ni(II) may be dominated by different sorption mechanisms. For example, at low pH values, cation exchange and inner-sphere surface complexation may be the main mechanisms. The oxygen-containing functional groups on biochar are protonated and Ni(II) ions are adsorbed through ion exchange between Ni^{2+} and Na^{+}/H^{+}. With an increase of pH, deprotonation occurs, resulting in the charge on the biochar surface changing from positive to negative. This process can benefit the sorption of the positively charged Ni(II) ions through electrostatic attraction. These mechanisms were also found in some other studies: the oxygen-containing groups (C-O, −OH, C = O) in oak bark biochars provided negatively charged surface sites (COO^{-} and OH^{-}) to attract Pb^{2+} (Mohan *et al.* 2007); pyrolysis of sugar beet tailings may yield electron-donor functional groups (C-OH, C-O, C-O-R), which can promote the sorption of chromium through reducing Cr(VI) to Cr(III) (Dong *et al.* 2011); some cationic nutrients such as Na, K, and Mg in oak and pine wood feedstock materials can increase the cation-exchange abilities of biochars and enhance Pb sorption through ion exchange at low pH values (Mohan *et al.* 2014).

According to the distribution of Ni(II) species calculated from the relative hydrolysis constants shown in Figure 4, it can be seen that Ni(II) exists in the species of Ni^{2+}, $Ni(OH)^{-}$, $Ni(OH)_2$, $Ni(OH)_3^{-}$, $Ni(OH)_4^{2-}$ at different pH values. At pH <8.8, Ni^{2+} is the predominant species. Therefore, the relatively low sorption of Ni^{2+} on biochar mainly arises from the competition between H^{+}/Na^{+} and Ni^{2+} on the biochar surface. In other words, Ni^{2+} is mainly removed through ion exchange. Similar results were found in many studies, which attribute them to the ion-exchange process (Tan *et al.* 2008a; Chen *et al.* 2016b).

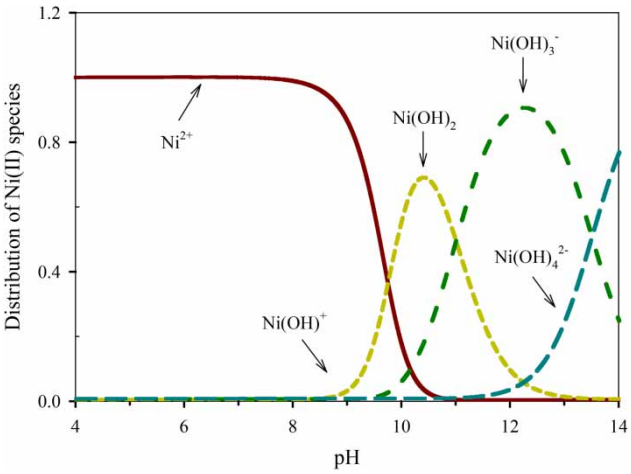

Figure 4 | The distribution of Ni(II) species as a function of pH values. $T = 293 \pm 2$ K, $C_{Ni(II)\ initial} = 10$ mg/L, $m/V = 0.45$ g/L.

As seen in Figure 3, there is no drastic difference in the Ni(II) sorption on biochar in the three different solution concentrations of $NaClO_4$ over the pH range of 4–11. The pH-dependent and ionic strength-independent sorption for Ni(II) ions suggests Ni(II) sorption on biochar is mainly due to inner-sphere surface complexation (Hayes & Leclie 1987). The precipitation curve of Ni(II) at the concentration of 10 mg/L is also shown in Figure 3. It is clear that Ni(II) starts to form a precipitate at pH ~8.8 if it is not adsorbed on biochar. At pH <8.8, the percentage of Ni(II) removal reaches its maximum value. Thus, Ni(II) removal from solution to biochar is not attributed to precipitation. Nevertheless, in view of the strong sorption of Ni(II) on biochar, the local Ni(II) concentration on the biochar surface is very high, and the formation of (co)precipitates on the biochar surface is also possible (Tan *et al.* 2014). Currently, the EXAFS technique provides insight into the formation of surface (co)precipitates and can help to distinguish the precipitates from inner-sphere surface complexes (Tan *et al.* 2008b). Therefore, further investigation is necessary at the molecular level to get an insight into the sorption mechanisms.

Effect of coexistent electrolyte ions

In practice, biochars derived from different materials display different sorption capacities and pathways for heavy metals under various aqueous conditions. In other words, the sorption process is determined by the identity of the adsorbent and the adsorbate, and the physicochemical conditions of the aqueous environment. To illustrate the effect of coexistent electrolyte ions on the sorption of Ni(II), the sorption behaviour of Ni(II) was investigated in multiple solutions as a function of the pH value and is shown in Figure 5. Ni(II) sorption on biochar is not affected by the electrolyte cations in the suspension, as can be seen from Figure 5(a). However, Chen *et al.* found the opposite result when investigating the sorption of Ni(II) on montmorillonite (Chen *et al.* 2016b). This effect of cations in solution on the sorption of heavy metals may be determined by different adsorbents. Thus, the role of cations in the sorption of Ni(II) on biochar is negligible over the entire pH range. The effect of ionic strength on the sorption of Ni(II) also proves that the sorption is chemical sorption and inner-sphere surface complexation rather than physical adsorption. Figure 5(b) shows

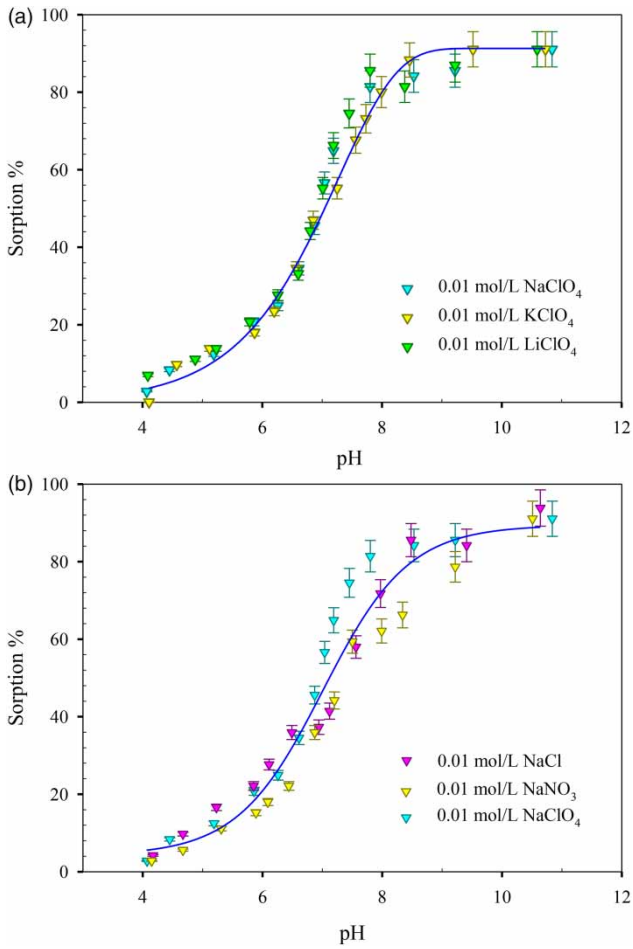

Figure 5 | Effect of coexistent electrolyte cations (a) and anions (b) on Ni(II) sorption on biochar surface at different pH values. $T = 293 \pm 2$ K, $C_{Ni(II)initial} = 10$ mg/L, $m/V = 0.45$ g/L.

the sorption of Ni(II) on biochar as a function of pH in 0.01 mol/L NaCl, $NaNO_3$, $NaClO_4$, respectively. These results demonstrate that there are no significant differences among the three electrolyte anions. Generally, the negatively charged anions can form complexes with the oxygen-containing groups on the surface of a solid. However, the influences of Cl^-, NO_3^-, and ClO_4^- on the sorption of Ni(II) are weak, suggesting that inner-sphere surface complexes are formed. This discovery is similar to Ni(II) sorption on montmorillonite (Chen *et al.* 2016b), U(VI) sorption on bentonite (Xiao *et al.* 2013), and Eu(III) sorption on graphene oxide (Hu *et al.* 2017a) but is different from Eu(III) sorption on titanate nanotubes (Sheng *et al.* 2012). This indicates that the sorption behaviour of a heavy metal is co-determined by the characters of the adsorbate, adsorbent, and environment. In addition, the mechanism of specific anions on biochar is difficult to distinguish using macroscopic investigation only. Thus, we need to further investigate related mechanisms at the molecular level to gain in-depth information.

Effect of solid content

Figure 6 illustrates the effects of the solid content on the Ni(II) sorption percent and sorption amount on biochar. One can see that the sorption percent increases from ~6% to 34% as the solid content increases from 0.1 g/L to 1.2 g/L. In general, the greater the applied solid content, the more available binding sites there are. Therefore, more Ni(II) ions can be bound with an increase in the solid content. It should be noted that the removal percent of Ni(II) on biochar reaches its highest level at $m/V > 0.9$ g/L. To reduce the purification cost of effluent, the appropriate content of biochar derived from rice straw to remove Ni(II) at pH 6.0 is 0.9 g/L.

As shown in Figure 6, the Ni(II) sorption amount decreases with rising biochar dosage. One possible reason is that the biochar particles disperse well in the solution at a lower solid dosage, which causes all the biochar surface sites to be exposed for more Ni(II) binding. Thereby, there is a higher sorption amount at a lower solid dosage. However, at a higher solid dosage, the collision among biochar particles can cause aggregation and decrease their dispersion ability in the solution. This process would reduce the total specific surface area and increase the path length of diffusion, finally resulting in the reduction of the availability of binding sites and Ni(II) sorption amount on biochar (Huang *et al.* 2008; Yang *et al.* 2010). In addition, some weak-linked Ni(II) on the biochar surfaces may be

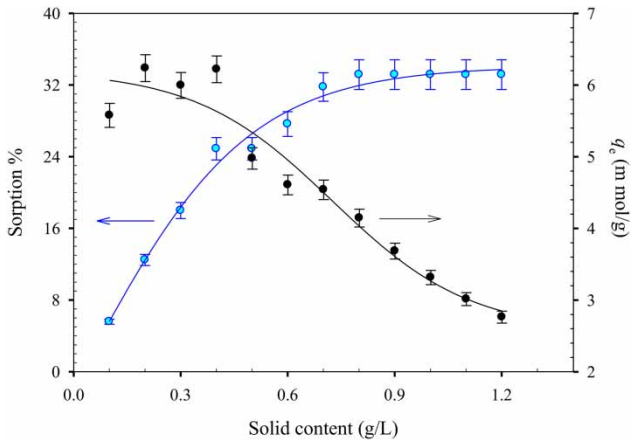

Figure 6 | Effect of solid content on the Ni(II) sorption percentage and Ni(II) sorption amount on biochar derived from rice straw. pH = 6.0 ± 0.2, $T = 293 \pm 2$ K, $C_{Ni(II)initial} = 10$ mg/L, I ($NaClO_4$) = 0.01 mol/L.

desorbed due to the collision between individual solid particles (Dong *et al.* 2014), which is also adverse to the sorption of Ni(II) on the biochar surface.

Effect of humic substances

Humic substances (HA/FA), ubiquitous in the natural environment, can mediate the sorption and transport of metal ions by forming complexes with metal ions (Sheng *et al.* 2016). Here, the pH-dependence of Ni(II) sorption on biochar in the absence and presence of HA/FA is shown in Figure 7. The presence of HA/FA enhances Ni(II) sorption on biochar at pH <7.2, it inhibits sorption at pH >7.2. There is no significant difference between the two sorption curves in the presence of HA and FA over the whole pH range. Similar effects of HA/FA have been found in many studies, including Ni(II) sorption on Na-attapulgite (Fan *et al.* 2009), Th(IV) sorption on NKF-6 zeolite (Wang *et al.* 2016), Eu(III) and UO_2^{2+} sorption on graphene oxide (Hu *et al.* 2017a, 2017b), and so on. These findings suggest the effects of HA/FA on sorption may be independent of the properties of adsorbents and the adsorbates but dependent on the pH of the solution. At low pH values, it is easy to attract the negatively charged HA/FA onto the positively charged biochar due to the stronger complexation ability between HA/FA and biochar compared with the ability between HA/FA and Ni(II). Subsequently, the electrostatic properties of the solid-aqueous interface are modified by the HA/FA adsorbed onto the biochar surface, which then provides a more favourable environment for Ni(II) sorption (Strathmann & Myneni 2005). Thereby, the addition of HA/FA enhances Ni(II) sorption at low pH values. However, at high pH values, the solubility of HA/FA increases and the charge on the biochar surface becomes negative, which causes the negatively charged HA/FA to be difficult to adsorb on the biochar surface. In addition, a part of the free stable HA/FA-Ni(II) complexes are formed in solution. Therefore, the sorption of Ni(II) on biochar significantly decreases at high pH values.

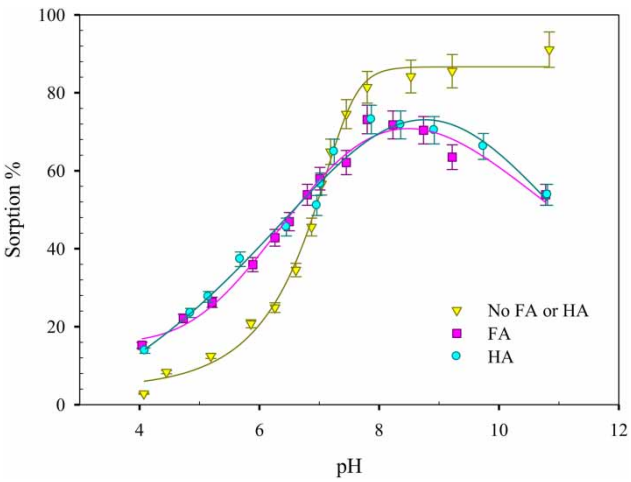

Figure 7 | Effect of both HA and FA on Ni(II) sorption onto biochar derived from rice straw. pH = 6.0 ± 0.2, T = 293 ± 2 K, $C_{Ni(II)initial}$ = 10 mg/L, I ($NaClO_4$) = 0.01 mol/L, m/V = 0.45 g/L.

Adsorption isotherms and thermodynamic study

Ni(II) sorption isotherms on biochar at 293, 313, and 333 K are show in Figure 8. The sorption amount of Ni(II) is the lowest at 293 K and highest at 313 K, indicating that high temperature is beneficial for the sorption of Ni(II) on biochar. To illustrate the sorption characteristics of Ni(II) on biochar, the Langmuir, Freundlich, and D-R models (Chen *et al.* 2016b) were simulated and the results are shown in Figure 8(a)–8(d). The linear forms of the three isotherm models can be expressed as follows:

$$\frac{C_e}{q_e} = \frac{1}{K_L q_{max}} + \frac{C_e}{q_{max}} \quad (2)$$

$$\log q_e = \log k_F + n \log C_e \quad (3)$$

$$\ln q_e = \ln q_{max} - \beta\varepsilon^2 \quad (4)$$

where q_{max} (mol/g) is the Ni(II) maximum sorption capacity on a per-weight basis of biochar; K_L (L/mol) is the Langmuir affinity parameter; K_F ($mol^{1-n}{\cdot}L^n/g$) and n represent the Freundlich affinity-capacity parameter and exponent, respectively; β is the D-R activity constant and ε is the Polanyi potential, which is calculated by $RT \ln(1 + 1/C_e)$. From the D-R model, the bonding energy of the ion-exchange mechanism (E, kJ/g) is calculated by $(2\beta)^{-1/2}$. Here, R is the universal gas constant [8.314 J/(K·mol)] and T (K) is the absolute temperature in kelvin.

The corresponding parameters of the three isotherms are also shown in Table 1. According to the curves of the simulated models and parameters listed in Table 1, it was found that the sorption isotherms fit very well to the three isotherm models. Especially for the Langmuir model, its regression coefficients of determination (R^2) are higher than those in the other two models, demonstrating that the Langmuir model best fits the isotherm. The result implies that the binding energies on the biochar are uniform and Ni(II) is adsorbed on the biochar surface by forming an almost complete monolayer coverage (Langmuir 1918). In addition, the values of q_{max} calculated from the Langmuir

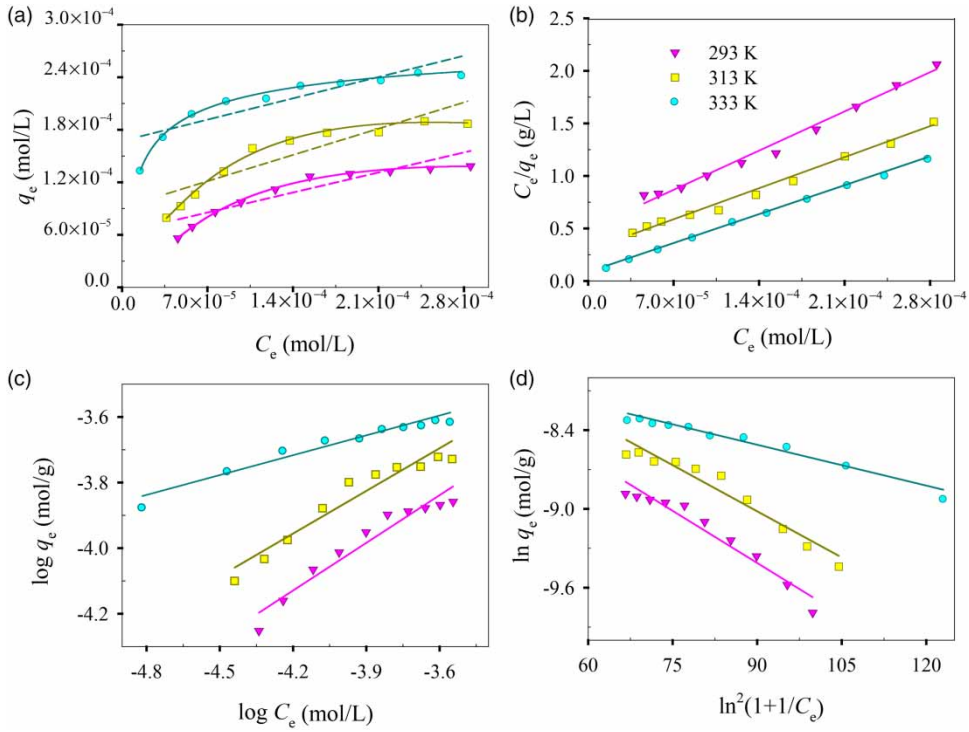

Figure 8 | Sorption isotherm (a), linearized Langmuir isotherm (b), linearized Freundlich isotherm (c), and linearized Dubinin-Radushkevich isotherm (d) for Ni(II) sorption onto biochar derived from rice straw at 293 K, 313 K, and 333 K. pH = 6.0 ± 0.2, $C_{Ni(II)initial}$ = 10–35 mg/L, I ($NaClO_4$) = 0.01 mol/L, m/V = 0.45 g/L.

Table 1 | The isotherm parameters derived from the Langmuir, Freundlich, and D-R models for Ni(II) sorption onto biochar at three temperatures. pH = 6.0 ± 0.2, $C_{Ni(II)initial}$ = 10 mg/L, I ($NaClO_4$) = 0.01 mol/L, m/V = 0.45 g/L

	Langmuir model		
T (K)	**q_{max} (mol/g)**	**b (L/mol)**	**R^2**
293	1.889×10^{-4}	3.811×10^{4}	0.9868
313	2.389×10^{-4}	8.408×10^{4}	0.9903
333	2.567×10^{-4}	3.736×10^{4}	0.9990
	Freundlich model		
T (K)	**K_F ($mol^{1-n} \cdot L^n/g$)**	**n**	**R^2**
293	7.741×10^{-3}	0.4806	0.9355
313	7.042×10^{-3}	0.4302	0.9313
333	1.300×10^{-3}	0.1994	0.9516
	D-R model		
T (K)	**q_{max} (mol/g)**	**β**	**R^2**
293	8.988×10^{-4}	0.0267	0.9481
313	1.003×10^{-3}	0.0236	0.9448
333	5.088×10^{-4}	0.0105	0.9678

model increase with an increase of temperature, which reveals that high temperature is beneficial to Ni(II) sorption on biochar. In the D-R model, the q_{max} values are different from the q_{max} values in Langmuir model. This discrepancy may be attributed to the different assumptions between the two models.

Here, Ni(II) maximum uptake capacity (i.e., q_{max}) of rice straw-derived biochar fitted by the Langmuir model was compared with the capacities of other sorbent materials. As displayed in Table 2, the q_{max} values of Ni(II) uptake on rice straw-derived biochar is greater than that of a series of materials including bagasse (Gupta *et al.* 2003), CMC-bentonite (Liu *et al.* 2012), Na-rectorite (Tan *et al.* 2008c), *Alternanthera philoxeroides* biomass (Wang & Qin 2006), *Phragmites australis* biochar (Liu *et al.* 2016), calcium-alginate (Huang *et al.* 1996), and magnetic nanoparticles (Sharma & Srivastava 2011), while it is lower than *Chrysanthemum indicum* biochar (Vilvanathan & Shanthakumar 2017) and *Citrus limetta* peel biochar (Vidhya *et al.* 2017). The result implies that rice straw-derived biochar is favourable but still needs a further-modified adsorbent to raise the sorption capacity. For example, another bio-sorbent (pine sawdust) exhibited an adsorption capacity more

Table 2 | Adsorption comparison of biochar and several reported materials for Ni(II)

Materials	q_{max} (mg/g)	References
Bagasse	1.70	Gupta *et al.* (2003)
CMC-bentonite	2.89	Liu *et al.* (2012)
Na-rectorite	7.18	Tan *et al.* (2008c)
Alternanthera philoxeroides biomass	9.73	Wang & Qin (2006)
Phragmites australis biochar	9.75	Liu *et al.* (2016)
Calcium-alginate	10.50	Huang *et al.* (1996)
Magnetic nanoparticles	11.53	Sharma & Srivastava (2011)
Rice straw biochar	11.96	This work
Chrysanthemum indicum biochar	29.44	Vilvanathan & Shanthakumar (2017)
Citrus limetta peel biochar	86.99	Vidhya *et al.* (2017)

than three times higher when it was modified by citric acid compared with the untreated pine sawdust (Zhou *et al.* 2015).

However, rice straw biochar has two prominent merits compared with the other two superior adsorbents: (1) the feedstock is easier to acquire; (2) it simultaneously solves the problem of environmental pollution from agriculture in China. In addition, the EPA provides the maximum contaminant levels (MCLs) of some heavy metals in ground water and drinking water, including lead (0.015 mg/L), mercury (0.002 mg/L), cadmium (0.005 mg/L), chromium (0.100 mg/L), zinc (5.000 mg/L), copper (1.300 mg/L), manganese (0.050 mg/L), and so on (Inyang *et al.* 2015). In this study, the rice-straw derived biochar can adsorb ~6.787 mg/L Ni (the maximum value simulated by Langmuir) from water. The data suggest that the biochar has the potential to meet the standard. Finally, it is noted that natural bio-sorbents are generally considered to be a cost-effective adsorbent alternatives for the removal of divalent heavy metal ions (Zhou *et al.* 2015). Therefore, rice straw-derived biochar deserves to be further explored as a new bio-sorbent.

To further investigate the thermodynamic properties of Ni(II) sorption on biochar, the sorption isotherms were employed to calculate the thermodynamic parameters. Gibbs free energy (ΔG^0) is calculated from the equation (Yang *et al.* 2011):

$$\Delta G^0 = -RT \ln K^0 \tag{5}$$

Table 3 | The thermodynamic parameters for Ni(II) sorption on biochar at three temperatures. pH = 6.0 ± 0.2, $C_{Ni(II)initial}$ = 10 mg/L, I ($NaClO_4$) = 0.01 mol/L, m/V = 0.45 g/L

T (K)	ΔG^0 (KJ/mg)	ΔS^0 [J/(mg·K)]	ΔH^0 (KJ/mg)
293	−17.810	15.763	13.191
313	−20.272		15.338
333	−24.114		18.865

where K^0 represents the equilibrium constant of the sorption reaction, and the values of $\ln K^0$ are obtained by plotting $\ln K_d$ versus C_e. Standard entropy (ΔS^0) and the average standard enthalpy (ΔH^0) are calculated from the slope and intercept of the plot of $\ln K^0$ versus 1/T, respectively (Li *et al.* 2012).

$$\ln K^0 = \frac{\Delta S^0}{R} - \frac{\Delta H^0}{RT} \tag{6}$$

The obtained thermodynamic parameters are listed in Table 3. The positive value of ΔH^0 indicates that the adsorption of Ni(II) on biochar is endothermic. In fact, the process of ions attaching to a solid surface is exothermic. However, the hydration sheaths of Ni(II) ions are partially destroyed in the sorption process, which requires energy (Chen & Wang 2006). Because the endothermic nature of the desolvation process exceeds that of the enthalpy of adsorption to a considerable extent, the final sorption is endothermic. The value of ΔG^0 is negative and becomes more negative as the temperature increases, implying that the sorption process is spontaneous and more efficient at higher temperatures. A positive value of ΔS^0 reflects the partial structural changes of Ni(II) and the biochar during the sorption process, leading to an increase in randomness at the biochar-solution interface. All the above analyses indicate that the sorption process of Ni(II) on biochar is spontaneous and endothermic.

CONCLUSIONS

In this paper, biochar derived from rice straw was characterized by using SEM, TEM, and FTIR. A batch technique was adopted to investigate the performance of biochar in the removal of Ni(II) as a function of various environmental conditions including pH, ion strength, foreign cations and anions, contact time, solid content, humic substances, and temperature. The sorption of Ni(II) on biochar rapidly reached equilibrium and kinetic studies suggested that the sorption can be well described by a pseudo-second-order

kinetic model. Ni(II) sorption was strongly dependent on pH but independent of ionic strength over the whole pH range. Ion exchange and inner-sphere surface complexation dominated the sorption process over the whole pH range. Solid content was also an important factor in controlling the sorption amount of Ni(II) on biochar and the appropriate content of biochar was 0.9 g/L. The effect of HA/FA on Ni(II) sorption was dependent on pH: the sorption was enhanced at low pH values but was reduced at high pH values. The thermodynamic data derived from temperature-dependent sorption isotherms suggested that the sorption of Ni(II) on biochar was an endothermic and spontaneous process. The above results are important for the application of biochar derived from rice straw to effluent management.

ACKNOWLEDGEMENTS

Financial support from the National Natural Science Foundation of China (31700476) is gratefully acknowledged.

REFERENCES

Bird, M. I., Wurster, C. M., de Paula Silva, P. H., Paul, N. A. & de Nys, R. 2011 Algal biochar: effects and applications. *GCB Bioenergy* **4**, 61–69.

Chen, C. L. & Wang, X. K. 2006 Adsorption of Ni(II) from aqueous solution using oxidized multi-walled carbon nanotubes. *Ind. Eng. Chem. Res.* **45**, 9144–9149.

Chen, C. L., Hu, J., Shao, D. D., Li, J. X. & Wang, X. K. 2009 Adsorption behavior of multiwall carbon nanotube/iron oxide magnetic composites for Ni(II) and Sr(II). *J. Hazard. Mater.* **164**, 923–928.

Chen, Y., Zhang, W., Yang, S., Hobiny, A., Alsaedi, A. & Wang, X. 2016a Understanding of the sorption mechanism of Ni(II) on grapheme oxides by batch experiments and density functional theory studies. *Sci. China Chem.* **4**, 412–419.

Chen, Z., Chen, L. & Lu, S. 2016b Effect of solution chemistry on the interaction of radionuclide ^{63}Ni(II) onto montmorillonite. *J. Radioanal. Nucl. Chem.* **308**, 505–516.

Ciosek, A. L. & Luk, G. K. 2017 Kinetic modelling of the removal of multiple heavy metallic ions from mine waste by natural zeolite sorption. *Water* **9**, 482.

Dong, X. L., Ma, L. N. Q. & Li, Y. C. 2011 Characteristics and mechanisms of hexavalent chromium removal by biochar from sugar beet tailing. *J. Hazard. Mater.* **190**, 909–915.

Dong, P., Wu, X., Sun, Z., Hu, J. & Yang, S. 2014 Removal performance and the underlying mechanisms of plasma-induced CD/MWCNT/iron oxides towards Ni(II). *Chem. Eng. J.* **256**, 128–136.

Fan, Q. H., Shao, D. D., Wu, W. S. & Wang, X. K. 2009 Effect of pH, ionic strength, temperature and humic substances on the sorption of Ni(II) to Na-attapulgite. *Chem. Eng. J.* **150**, 188–195.

Gautam, P. K., Gautam, P. K., Banerjee, S., Soni, S., Singh, S. K. & Chattopadhyaya, M. C. 2015 Removal of Ni(II) by magnetic nanoparticles. *J. Mol. Liq.* **204**, 60–69.

Gupta, S. S. & Bhattacharyya, K. G. 2006 Adsorption of Ni(II) on clays. *J. Colloid Interf. Sci.* **295**, 21–32.

Gupta, V. K., Jain, C. K., Ali, I., Sharma, M. & Saini, V. K. 2003 Removal of cadmium and nickel from wastewater using bagasse fly ash – a sugar industry waste. *Water Res.* **37**, 4038–4044.

Hayes, K. F. & Leclie, J. O. 1987 Modeling ionic strength effect on cation adsorption at hydrous oxide/solution interfaces. *J. Colloid Interf. Sci.* **115**, 564–572.

Ho, Y. 2006 Review of second-order models for adsorption systems. *J. Hazard. Mater.* **37**, 681–689.

Ho, Y. & McKay, G. 1999 Pseudo-second order model for sorption processes. *Process Biochem.* **34**, 451–465.

Hu, B., Hu, Q., Li, X., Pan, H., Tang, X., Chen, C. & Huang, C. 2017a Rapid and highly efficient removal of Eu(III) from aqueous solutions using graphene oxide. *J. Mol. Liq.* **229**, 6–14.

Hu, B., Hu, Q., Li, X., Pan, H., Huang, C. & Chen, C. 2017b Graphene oxide as a novel adsorbent for highly efficient removal of UO_2^{2+} from water. *Desalin. Water Treat.* **79**, 178–187.

Huang, C., Chung, Y. C. & Liou, M. R. 1996 Adsorption of Cu(II) and Ni(II) by pelletized biopolymer. *J. Hazard. Mater.* **45**, 265–277.

Huang, J. H., Liu, Y. F. & Wang, X. G. 2008 Selective sorption of tannin from flavonoids by organically modified attapulgite clay. *J. Hazard. Mater.* **160**, 382–387.

Inyang, M. I., Gao, B., Yao, Y., Xue, Y., Zimmerman, A., Mosa, A., Pullammanappallil, P., Sik Ok, Y. & Cao, X. 2015 A review of biochar as a low-cost adsorbent for aqueous heavy metal removal. *Crit. Rev. Env. Sci. Tec.* **46**, 406–433.

Kadirvelu, K., Thamaraiselvi, K. & Namasivayam, C. 2001 Adsorption of nickel(II) from aqueous solution onto activated carbon prepared from coirpith. *Sep. Purif. Technol.* **24**, 497–505.

Kasprzak, K. S., Sunderman Jr, F. W. & Salnikow, K. 2003 Nickel carcinogenesis. *Mutat. Res.* **533**, 67–97.

Kołodyńska, D., Krukowska, J. & Thomas, P. 2017 Comparison of sorption and desorption studies of heavy metal ions from biochar and commercial active carbon. *Chem. Eng. J.* **307**, 353–363.

Langmuir, I. 1918 The adsorption of gases on plane surfaces of glass, mica and platinum. *J. Am. Chem. Soc.* **40**, 1361–1403.

Li, J., Zhang, S., Chen, C., Zhao, G., Yang, X., Li, J. & Wang, X. 2012 Removal of Cu(II) and fulvic acid by graphene oxide nanosheets decorated with fe_3o_4 nanoparticles. *ACS Appl. Mater. Inter.* **4**, 4991–5000.

Liang, X., Xu, Y., Sun, G., Wang, L., Sun, Y., Sun, Y. & Qin, X. 2011 Preparation and characterization of mercapto functionalized sepiolite and their application for sorption of lead and cadmium. *Chem. Eng. J.* **174**, 436–444.

Liu, Z. J., Yang, J. W., Zhang, Z. C., Chen, L. & Dong, Y. H. 2012 Study of ^{63}Ni(II) sorption on CMC-bound bentonite from aqueous solutions. *J. Radioanal. Nucl. Chem.* **291**, 801–809.

Liu, P., Yue, M. & Zhang, H. 2016 Adsorption performance of Ni(II) from aqueous solutions using biochar made of *Phragmites australis* by adding ammonium polyphosphate as flame retardant. *J. Chem.* **2016**, 1797396.

Malkoc, E. & Nuhoglu, Y. 2005 Investigation of nickel(II) removal from aqueous solutions using tea factory waste. *J. Hazard. Mater.* **127**, 120–128.

Mohan, D., Pittman Jr, C. U., Bricka, M., Smith, F., Yancey, B., Mohammad, J., Steele, P. H., Alexandre-Franco, M. F., Gómez-Serrano, V. & Gong, H. 2007 Sorption of arsenic, cadmium, and lead by chars produced from fast pyrolysis of wood and bark during bio-oil production. *J. Colloid Interf. Sci.* **310**, 57–73.

Mohan, D., Kumar, H., Sarswat, A., Alexandre-Franco, M. & Pittman Jr, C. U. 2014 Cadmium and lead remediation using magnetic oak wood and oak bark fast pyrolysis bio-chars. *Chem. Eng. J.* **236**, 513–528.

Panneerselvam, P., Morad, N. & Tan, K. A. 2011 Magnetic nanoparticle (Fe_3O_4) impregnated onto tea waste for the removal of nickel(II) from aqueous solution. *J. Hazard. Mater.* **186**, 160–168.

Sharma, Y. C. & Srivastava, V. 2011 Comparative studies of removal of Cr(VI) and Ni(II) from aqueous solutions by magnetic nanoparticles. *J. Chem. Eng. Data* **56** (2011), 819–825.

Sheng, G., Yang, S., Sheng, J., Hu, J., Tan, X. & Wang, X. 2011 Macroscopic and microscopic investigation of Ni(II) sequestration on diatomite by batch, XPS and EXAFS techniques. *Environ. Sci. Technol.* **45**, 7718–7726.

Sheng, G., Yang, S., Zhao, D., Sheng, J. & Wang, X. 2012 Adsorption of Eu(III) on titanate nanotubes studied by a combination of batch and EXAFS technique. *Sci. China Chem.* **55**, 182–194.

Sheng, G., Alsaedi, A., Shammakh, W., Monaquel, S., Sheng, J., Wang, X., Li, H. & Huang, Y. 2016 Enhanced sequestration of selenite in water by nanoscale zero valent iron immobilization on carbon nanotubes by a combined batch, XPS and XAFS investigation. *Carbon* **99**, 123–130.

Strathmann, T. & Myneni, S. 2005 Effect of soil fulvic acid on nickel(II) sorption and bonding at the aqueous-boehmite (γ-AlOOH) interface. *Environ. Sci. Technol.* **39**, 4027–4034.

Tan, X. L., Hu, J., Zhou, X., Yu, S. M. & Wang, X. K. 2008a Characterization of Lin'an montmorillonite and its application in the removal of Ni^{2+} from aqueous solutions. *Radiochim. Acta* **96**, 487–495.

Tan, X. L., Wang, X. K., Geckeis, H. & Rabung, T. 2008b Sorption of Eu(III) on humic acid or fulvic acid bound to alumina studied by SEM-EDS, XPS, TRLFS and batch techniques. *Environ. Sci. Technol.* **42**, 6532–6537.

Tan, X. L., Chen, C. L., Yu, S. M. & Wang, X. K. 2008c Sorption of Ni^{2+} on Na-rectorite studied by batch and spectroscopy methods. *Appl. Geochem.* **23**, 2767–2777.

Tan, X. L., Fang, M., Ren, X. M., Mei, H. Y., Shao, D. D. & Wang, X. K. 2014 Effect of silicate on the formation and stability of Ni-Al LDH at γ-Al_2O_3 surfaces. *Environ. Sci. Technol.* **48**, 13138–13145.

Tang, W. W., Zeng, G. M., Gong, J. L., Liang, J., Xu, P., Zhang, C. & Huang, B. B. 2013 Impact of humic/fulvic acid on the removal of heavy metals from aqueous solutions using nanomaterials: a review. *Sci. Total Environ.* **468–469**, 1014–1027.

Tong, X. J., Li, J. Y., Yuan, J. H. & Xu, R. K. 2011 Adsorption of Cu (II) by biochars generated from three crop straws. *Chem. Eng. J.* **172**, 828–834.

Vidhya, L., Dhandapani, M. & Shanthi, K. 2017 Sequestering divalent nickel ions from aqueous solution using activated carbon of *Citrus limetta* peel: isothermic and kinetic studies. *Pol. J. Environ. Stud.* **26**, 1737–1745.

Vilvanathan, S. & Shanthakumar, S. 2017 Ni (II) adsorption onto *Chrysanthemum indicum*: influencing factors, isotherms, kinetics, and thermodynamics. *Int. J. Phytoremediat.* **18**, 1046–1059.

Wang, X. S. & Qin, Y. 2006 Removal of Ni(II), Zn(II) and Cr(VI) from aqueous solution by *Alternanthera philoxeroides* biomass. *J. Hazard. Mater.* **138**, 582–588.

Wang, J., Chen, Z., Chen, W., Li, Y., Wu, Y., Hu, J., Alsaedi, A., Alharbi, N. S., Dong, J. & Linghu, W. 2016 Effect of pH, ionic strength, humic substances and temperature on the sorption of Th(IV) onto NKF-6 zeolite. *J. Radioanal. Nucl. Chem.* **310**, 597–609.

Xiao, J., Chen, Y., Zhao, W. & Sorption, X. J. 2013 Behavior of U(VI) onto Chinese bentonite: effect of pH, ionic strength, temperature and humic acid. *J. Mol. Liq.* **188**, 178–185.

Yang, S. T., Zhao, D. L., Zhang, H., Lu, S. S., Chen, L. & Yu, X. J. 2010 Impact of environmental conditions on the sorption behavior of Pb(II) in Na-bentonite suspensions. *J. Hazard. Mater.* **183**, 632–640.

Yang, S. T., Sheng, G. D., Tan, X. L., Hu, J., Du, J. Z., Montavon, G. & Wang, X. K. 2011 Determination of Ni(II) uptake mechanisms on mordenite surfaces: a combined macroscopic and microscopic approach. *Geochim. Cosmochim. Acta* **75**, 6520–6534.

Zhou, Y., Lu, P. & Lu, J. 2012 Application of natural biosorbent and modified peat for bisphenol a removal from aqueous solutions. *Carbohyd. Polym.* **88**, 502–508.

Zhou, Y., Zhang, R., Gu, X. & Lu, J. 2015 Adsorption of divalent heavy metal ions from aqueous solution by citric acid modified pine sawdust. *Sep. Sci. Technol.* **50**, 245–252.

Zhou, Y., Fang, X., Wang, K., Hu, Y., Chen, K. & Lu, J. 2017 Improving cyanide removal from coke plant wastewaters by optimizing the operation conditions of an ammonia still tower. *Energ. Source. Part A* **39**, 491–496.

Zong, P., Wang, H., Pan, H., Zhao, Y. & He, C. 2013 Application of NKF-6 zeolite for the removal of U(VI) from aqueous solution. *J. Radioanal. Nucl. Chem.* **295**, 1969–1979.

First received 11 August 2017; accepted in revised form 16 May 2018. Available online 7 June 2018